Yi Xiong[1]
Digital Manufacturing and Design Centre,
Singapore University of Technology and Design,
Singapore 487372, Singapore
e-mail: yi_xiong@sutd.edu.sg

Pham Luu Trung Duong
Digital Manufacturing and Design Centre,
Singapore University of Technology and Design,
Singapore 487372, Singapore
e-mail: luu_pham@sutd.edu.sg

Dong Wang
Robotics Institute,
School of Mechanical Engineering,
State Key Laboratory of Mechanical System and
Vibration, Shanghai Jiao Tong University,
Shanghai 200241, China
e-mail: wang_dong@sjtu.edu.cn

Sang-In Park
Department of Mechanical Engineering
and Robotics,
Incheon National University,
Incheon 22012, South Korea
e-mail: sangin.park@inu.ac.kr

Qi Ge
Science and Math Cluster and
Digital Manufacturing and Design Centre,
Singapore University of Technology and Design,
Singapore 487372, Singapore
e-mail: ge_qi@sutd.edu.sg

Nagarajan Raghavan
Engineering Product Development Pillar and
Digital Manufacturing and Design Centre,
Singapore University of Technology and Design,
Singapore 487372, Singapore
e-mail: nagarajan@sutd.edu.sg

David W. Rosen
Digital Manufacturing and Design Centre,
Singapore University of Technology and Design,
Singapore 487372, Singapore;
The G. W. Woodruff School of
Mechanical Engineering,
Georgia Institute of Technology,
Atlanta, GA 30332
e-mail: david_rosen@sutd.edu.sg

Data-Driven Design Space Exploration and Exploitation for Design for Additive Manufacturing

Recently, design for additive manufacturing has been proposed to maximize product performance through the rational and integrated design of the product, its materials, and their manufacturing processes. Searching design solutions in such a multidimensional design space is a challenging task. Notably, no existing design support method is both rapid and tailored to the design process. In this study, we propose a holistic approach that applies data-driven methods in design search and optimization at successive stages of a design process. More specifically, a two-step surrogate model-based design method is proposed for the embodiment and detailed design stages. The Bayesian network classifier is used as the reasoning framework to explore the design space in the embodiment design stage, while the Gaussian process regression model is used as the evaluation function for an optimization method to exploit the design space in detailed design. These models are constructed based on one dataset that is created by the Latin hypercube sampling method and then refined by the Markov Chain Monte Carlo sampling method. This cost-effective data-driven approach is demonstrated in the design of a customized ankle brace that has a tunable mechanical performance by using a highly stretchable design concept with tailored stiffnesses. [DOI: 10.1115/1.4043587]

1 Introduction

Additive manufacturing (AM) technologies enable the realization of engineering products that are rich in shape, material, hierarchical, and functional complexities [1]. For example, the state-of-the-art multimaterial AM machine can fabricate a part that is composed of millions of voxels in which each one can have its own designed material composition. Design for additive manufacturing (DfAM), a new methodology that evolves from design for manufacturing (DfM), is therefore proposed to harness these untapped potentials brought by AM. In DfAM, manufacturing constraints in conventional manufacturing processes have been greatly relaxed due to AM's layer-based, additive nature opening up new design freedoms; however, new challenges have arisen in design search and optimization given the increased number of design variables and their complicated interactions over multiple domains.

To accommodate all design variables and reflect their interactions, previous studies [1,2] proposed a design problem formulation for computer-aided design (CAD) using the process-structure-property (PSP) linkage, as shown in Fig. 1. For instance, in the selective laser melting (SLM) process, PSP relationships for metals often relate process conditions, such as melt pool temperature, to microstructure characteristics, such as grain size and shape, to mechanical properties such as hardness and fracture energy. Moreover, the PSP

[1]Corresponding author.

Contributed by the Design Theory and Methodology Committee of ASME for publication in the Journal of Mechanical Design. Manuscript received January 8, 2019; final manuscript received April 10, 2019; published online May 23, 2019. Assoc. Editor: Ying Liu.

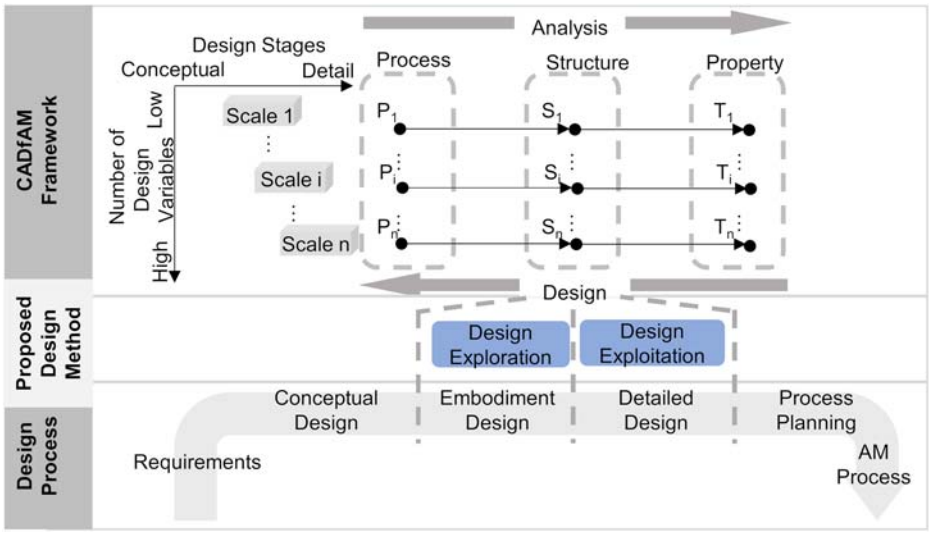

Fig. 1 (Top) The process-structure-property-based design problem formulation for a computer-aided design for AM system proposed in Ref. [1]; (bottom) the design process for AM-fabricated products that adapt from Ref. [3]; and (middle) the proposed design method for design exploration in embodiment design and for design exploitation in detailed design

linkage is also found at various scales ranging from material microstructure to part macrostructure. The specific focus in this paper is on how to represent and utilize process-structure-property relationships in embodiment and detailed design. That is, given a design concept, our proposed design method explores configurations of complex geometric structures and/or material compositions to satisfy performance requirements. Based on the analyses of typical design scenarios, requirements for design methods that support this view of the design for additive manufacturing are summarized in Table 1. Such requirements intend to serve as general guidelines for the development of design methods for AM. Accordingly, the proposed solutions in this study are also listed for each requirement.

In general, it is desired that the method is both rapid and tailored to meet requirements at different stages of design. First, it is impossible to search for such an enlarged design space without a rapid design method. As the optimal solution is often nonunique, the search must simultaneously consider all design variables and thoroughly examine the entire design space. As discussed in Ref. [4], products with desired properties can be achieved through designs of its material composition, geometric structure, or manufacturing process. Second, the design method also needs to be tailored to the design process. Reference [3] defined a design process with four steps: requirement clarification, conceptual design, embodiment design, and detailed design, as shown in Fig. 1. In embodiment design, designers determine the overall layout design, the preliminary form design, and the production processes based on design feasibility checks which are also called design space exploration. These decisions have a significant impact on the whole product lifecycle since subsequent changes may entail high costs or may be impossible. Design space exploration searches for a set of potential solutions to meet design targets that are defined by a set of ranges rather than specific values. In detailed design, design exploitation narrows a set of potential solutions obtained from design exploration down to one optimal design and provides ready-to-execute instructions. Therefore, design methods utilized for navigating PSP relationships must consider different requirements between design exploration and exploitation in a design process.

Table 1 Characteristics of DfAM, their requirements for the design method, and proposed solutions

Characteristics of DfAM	Requirements for the design method	Proposed solutions
A large number of design variables	Rapid design methods	• Data-driven methods
Design variables are at various scales and in different domains	Able to solve multidisciplinary optimization/multiscale optimization problems	• Set-based exploration • Data-driven methods
Multiple design objectives	Able to solve multiobjective optimization problems	• Set-based exploration
Mass customization	Allow reuse of embodiment design information in detailed design for each customized target	• Two-step sampling approach • Classification and regression models

However, there is no existing design method that meets all these requirements. This paper addresses this research gap by introducing data-driven models as the reasoning framework that supports mappings between the design space and performance space at different stages of the design process. The use of data-driven methods allows computationally expensive physical-based simulation models, e.g., finite element (FE) analysis and computational fluid dynamics, to be replaced by simple models, trained from datasets, that approximate relationships between two spaces. The computational efficiency of data-driven models allows more comprehensive and efficient design space search especially for complex and high-dimensional design problems.

In the context of design for additive manufacturing, existing works that utilized data-driven methods are found primarily for process planning applications [5–7]. Meanwhile, few studies have investigated the potential of using data-driven models in the design process of additively manufactured products [8,9]. In general, previous research does not take a holistic approach to data-driven DfAM methods nor does it enable the consideration of different requirements at different design stages. Moreover, such a lack of an integrated data flow is also found in existing data-driven design methods for more general engineering cases, which are reviewed in Sec. 2. These works either focus on applications in design space exploration or in design exploitation which overlook the possible linkage between them. The potential to reuse the information obtained from embodiment design in detailed design is of

great significance for the design for additive manufacturing. For instance, to meet various customized requirements, the design of AM products, e.g., footwear and tooth aligner, often involves frequent and minor changes of design targets during detailed design; meanwhile, their embodiment designs are often identical.

The main objective of this study is to propose a data-driven model-based method for both design space exploration and exploitation in the context of design for additive manufacturing. We propose a two-step design strategy: the Bayesian network classifier (BNC)-based approach proposed by Seepersad et al. [10,11] is adapted in design exploration for embodiment design. The Gaussian process regression (GPR) model is used as the evaluation function in optimization to exploit the design space for detailed design. These models are constructed based on one dataset that is created by the Latin hypercube sampling method and then refined by the Markov Chain Monte Carlo (MCMC) sampling method.

The main contribution of this research is threefold. First, specific requirements for methods to explore and exploit the design space enabled by additive manufacturing are identified. Second, in response to these requirements, existing methods to support the design process are integrated into a two-step data-driven model-based design method that includes the BNC-based exploration method, GPR-based exploitation method, and MCMC-based resampling strategy. Design information is gradually increased in the sequential design decision-making process. Lastly, datasets, instead of models, carry all design information accumulated at different design stages, which allow keeping design freedom to the later stages of design and delay design commitment under insufficient information. The design information can also be shared among different design teams in concurrent design without disclosing the details of models. One should note that the proposed method is presented in the context of DfAM, the method appears to be applicable for solving a broad range of engineering design problems.

The rest of this paper is structured as follows. Section 2 reviews the existing work on design exploration and exploitation. In Sec. 3, data-driven methods and models used in this work are introduced. In Sec. 4, a two-step data-driven model-based design method is proposed for the design for additive manufacturing. To demonstrate the proposed framework, an exemplified case of a customized ankle brace design is presented in Sec. 5. Conclusions are drawn in Sec. 6.

2 Design Space Exploration and Exploitation Methods

2.1 Overview. To support informed decision-making in design, it is crucial that engineers have a correct understanding of relationships between design variables and product performance. However, setting up such linkages is nontrivial since modern design problems, e.g., design for additive manufacturing, typically have many design variables and their interactions are complicated and unclear. Design exploration and exploitation, as two different strategies to provide insight into the design space, are often adopted by designers at different stages of the design process. Detailed comparisons between the two strategies are summarized in Table 2.

The past 30 years have witnessed growing research on the model-based design exploration and exploitation because alternatives such as experimental or empirical approaches are low-efficient and costly. Table 3 presents a literature survey of existing model-based methods and tools. Applications are found at different stages of the design process, particularly in embodiment and detailed design stages. Few cases [12–14] are found in the conceptual design stage due to the following reasons: (1) high-level functional/behavior models instead of low-level physical models are typically used for searching engineering principles and solutions and (2) the design decisions are made with enumerative approaches [15] rather than the exploitation and exploration approaches. It is apparent from Table 3 that existing methods focus on one-design stage and have not considered an integrated method to connect different stages. The rest of this section reviews existing methods for each stage in detail. Based on these summaries, Sec. 4 presents a data-driven two-step approach to use design exploration and exploitation together.

Table 2 Comparisons between design exploration and design exploitation

	Design exploration	Design exploitation
Targets	Quickly identify all design alternatives that satisfy a range of design target	Search for a design with maximum performance for defined criteria
Design stages	Conceptual design/ embodiment design	Detailed design
Strategies	• Identify the domain boundary of feasible designs • Maximize the minimum distance among sampling points to explore as many designs as possible	• Start with an initial design and iteratively modify it to maximize the performance • The design is modified according to acquisition functions, e.g., gradient information, expected improvement
Design outputs	A set of potential designs	One optimal design

2.2 Existing Design Exploration Methods. Design exploration aims to identify all design alternatives that satisfy a range of design targets, especially these unique, optimal, and undiscovered ones. These feasible designs are sets of bounded regions in the design space, and their boundaries represent various constraints in a design process, e.g., performance requirements and manufacturability. These boundaries are expressed with explicit or implicit methods. The explicit method utilizes either intervals or visualization tools to define boundaries. However, intervals are not able to express these disconnected, arbitrarily shaped feasible regions. Meanwhile, visualization tools are not effective for the high-dimensional design space. To tackle the above limitations, the implicit method stores the boundary information as models, e.g., classifiers, and evaluates the feasibility of untested design based on these models.

One central task of design exploration is the identification of boundaries between feasible and infeasible designs. Existing approaches can be divided into two categories: exhaustive search and statistical inference. In the exhaustive search approach, the design space is divided into hypercubes and each candidate is evaluated through computer simulations or experiments. The size of the hypercube is determined by the required resolution. Some examples of the exhaustive search approach are inductive design exploration method [18] and surrogate-assisted illumination method [9]. Although parallel computing is allowed in this method, the total computational cost is very expensive. In addition, the exhaustive method often represents the domain boundary using explicit methods.

In the statistical inference approach, probabilistic models are used to estimate the boundary based on a small number of evaluated designs. The posterior class probability of each candidate design is generated based on the Bayes' rule. A design is considered feasible if its posterior probability for the class of feasible designs is over a predefined threshold. Examples have been demonstrated with the Bayesian network classifier [9–11] and Gaussian process classifier [25]. In a series of work by Seepersad and co-workers, a set-based design space exploration method was proposed in Refs. [9–11]. Bayesian network classifiers were introduced to map complex, disjoint, arbitrarily shaped region of interest in a multidimensional design space at different scales. This method was demonstrated in various applications including the design of metamaterials with negative stiffness [10], and the design of mechanical components with spatially controlled mechanical properties [4]. Recently, the set-based method has been further expanded to consider

Table 3 A literature survey of research on model-based design exploration and exploitation

Authors	Methods		Design stages		
	Models	Sampling and reasoning tools	Cnpt.	Embd.	Detl.
Malak et al. [12]	Low-fidelity	• Multiattribute utility theory • Set-based design	√	–	–
Finger and co-workers [13,14]	GPR	• Multistage Bayesian surrogate methodology • Maximum entropy sampling	√	–	–
Unal et al. [16]	High-fidelity and bounding models	• Formal model of sequential design	–	√	–
Chen et al. [17]	RSM	• Taguchi method (small noise) • Suh's design axioms • Compromise decision support problem	–	√	–
Choi et al. [18]	High-fidelity	• Full factorial sampling plan • Hyperdimensional error margin indices	–	√	–
Seepersad and co-workers [9–11,19]	BNC	• Bayesian network classifiers: Naïve Bayes classifier and Parzen Window classifier	–	√	–
Gaier et al. [20]	GPR	• Multidimensional archive phenotypic elites	–	√	–
Larson and Mattson [21]	GPR	• Expected improvement criterion	–	√	–
Chen and Fuge [25]	GPC	• e-margin sampling	–	√	–
Couckuyt et al. [22]	GPR	• Expected improvement criterion • Surrogate-based optimization	–	–	√
Simpson and Mistree [23]	GPR	• Surrogate-based optimization	–	–	√
Qian et al. [24]	GPR	• Multifidelity surrogate models • Surrogate-based optimization	–	–	√

uncertainties from additive manufacturing processes, e.g., micro-stereolithography [9]. Also, existing work identified the boundary within a given bounded design volume; however, exploring unbounded design space is also receiving growing attention [25]. In this study, a statistical inference approach is used to determine sets of feasible designs and their boundaries are represented with the implicit method.

2.3 Existing Design Exploitation Methods. Design exploitation searches for a single optimal design using well-established optimization techniques, such as gradient, stochastic, and heuristic methods. As discussed, data-driven models are often used as evaluation functions in optimization to reduce computation time. Many studies of data-driven model-based optimization can be found in the engineering design literature [26,27]. For DfAM, Ref. [7] demonstrated the feasibility of using data-driven models such as regression trees and GPR models in the process parameter optimization of the SLM process for fabricating parts with desired properties, such as high density. Using a similar approach, Ref. [5] utilized GPR models in the SLM process to identify processing windows that avoid the keyhole mode in the melt pool. In the fused deposition modeling process, Ref. [6] utilized a functional Gaussian process-based surrogate model that trained from FE thermal simulations to predict thermal fields of parts in the fabrication process.

Here, we discuss two important aspects of data-driven model-based optimization: model selection and sampling plan. Various models including neural networks, response surfaces, GPR models, etc., have been used in the model-based optimization. It is risky to advocate any model over another because their performance is case-specific. However, GPR models are clearly a popular choice for design exploitation and the reason is threefold. First, different than other metamodels, GPR models can give not only a point prediction about the untested input but also a quantitative confidence level regarding the prediction. The information of the confidence level can be either used to improve the accuracy of the model or provide some criteria in the design for robustness. In addition, GPR models require only a small dataset for fitting to generate accurate predictions. Lastly, various GPR models have been widely studied, the modified GPR models such as Co-Kriging models and Stochastic Kriging models are well-established to solve various types of problems, e.g., data from multifidelity sources, noisy data with heterogeneous variances.

On the other hand, the sampling plan plays a crucial role in data-driven model-based optimization. As a compromise to reduce the computational cost, data-driven models are often approximations of high-fidelity models and their accuracies therefore need to be considered. Based on the arrangement of sampling points, the sampling strategy is classified as global sampling or local sampling. The sampling method used in the design exploration stage of this study is a global sampling approach. In contrast, a local sampling approach is used in the design exploitation stage of the proposed framework. On the other hand, the sampling strategy, depending on the sequence of data generation, is categorized into two types: the one-shot approach and sequential approach. The one-shot approach generates all sampling points, and one static data-driven model is used in the optimization. If extra computer simulations or experiments are allowed in the optimization, a sequential sampling approach is often employed in optimization iterations to improve the model accuracy. The sequential sampling approach can be further classified as point sequential and batch sequential design. The point sequential approach fetches one new design point per time to evaluate and utilizes the updated dataset to train the data-driven model. This approach does not allow parallel evaluations and cannot be used to decouple complex design problems. Meanwhile, the batch sequential design approach selects several new design points to refine the dataset and model in a more efficient approach. In this study, a two-step batch sequential-based local sampling approach is used for design exploitation.

3 Data-Driven Methods and Models

This section first presents the data-driven method in a general form and then introduces two specific models. Specifically, the Bayesian network classifier, as a type of classification models, is explained; and the Gaussian process regression, as a type of regression models, is elucidated.

3.1 Data-Driven Methods. Data-driven models, as called as surrogate models or metamodels, are utilized in this study as the reasoning framework that offers a rapid method for design space exploration and exploitation. These models replace computationally expensive high-fidelity models by approximating their input–output behavior with training datasets. For engineering design, the term input–output behavior specifically refers to the mapping between

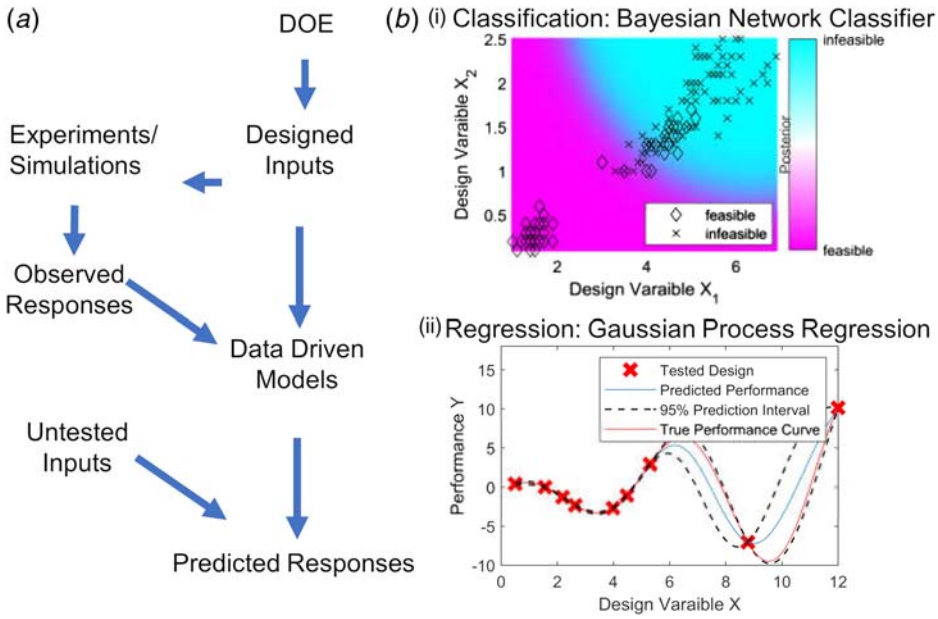

Fig. 2 (*a*) Training of data-driven models and (*b*) examples of data-driven models: (*i*) classification: Bayesian network classifiers that classify the design space into feasible and infeasible parts based on the dataset of observed inputs and responses and (*ii*) regression: Gaussian process regression models that predict the responses at untested design sets based on the observed dataset. Also, the 95% prediction interval is given as dash lines.

design variables and their performance. As shown in Fig. 2(*a*), the use of a data-driven method comprises three steps: training dataset collection, model fitting, and model evaluation.

Training datasets are collected from experiments, simulations, or both. This study focuses on the dataset collected by evaluating design points using high-fidelity simulations. Since data-driven models predict the response of unevaluated input based on its locality relationship with evaluated points, the selection strategy for these design points has a direct influence on the accuracy of models. Typical simulation-based DoE methods include Latin hypercube sampling and quasi-Monte Carlo sampling. It should be noted that the DoE method for deterministic computer simulations does not consist of replications, which are often included in the classical experiment-based DoE method.

Once the dataset is collected, the next step is to select suitable data-driven models for the design process. In general, data-driven models can be classified based on their applications as three categories: clustering, classification, and regression. Clustering models group a set of design points to a given number of clusters, and it is widely used for model reductions. Both classification and regression models belong to supervised learning and map inputs to outputs based on the training input–output pairs. If outputs are discrete values, the model is a classification model, and if outputs are continuous values, the model is a regression model. The classification model is suitable for design space exploration in embodiment design, which aims to divide the design space into feasible and infeasible space. Meanwhile, the regression model can be used for the design space exploitation in detailed design that requires intensive design evaluations.

Selected models are built to best-fit training data. Parameters of models are estimated using the optimization algorithm according to a set of measures (e.g., the maximum likelihood estimation and cross-validation). The optimization iteration continues until the model meets the predefined criterion and returns final data-driven models. If no criterion is met and new training data collection is possible, subsequent new training data are collected using an adaptive sampling approach. The new dataset can be used to improve both the global and local performance of data-driven models.

In this work, the above three-step training process is applied to the BNC and GPR. Meanwhile, the data collected during the training of BNC in design exploration are reused as a part of training data for the GPR model in design exploitation. Comprehensive reviews regarding DoE methods, model selections, and adaptive sampling methods can be found in Refs. [26,27].

3.2 Bayesian Network Classifier. Bayesian network classifiers are probabilistic classifier based on Bayes' theorem that predicts the class of untested inputs based on examples of the labeled data. Design exploration only considers a binary classification problem in which the input is classified as either feasible (denoted as class 1) or infeasible (denoted as class 2). The posterior probability of a class $k = 1$ or 2 is estimated as

$$p(c_k|x) = \frac{p(x|c_k)p(c_k)}{\sum_{m=1}^{2} p(x|c_m)p(c_m)} \tag{1}$$

where $p(c_k)$ is the prior probability for class c_k and $p(x|c_k)$ is the conditional probabilities. The prior probability is estimated based on the observations using $p(c_k) = (N_k + \lambda)/N + 2*\lambda$, where N_k is the number of observations that belongs to the class k from the total N observations and the Laplace smoothing factor $\lambda = 1$. The task of training the classifier becomes estimating $p(x|c_k)$, which can be assumed as various types of distributions. This study considers $p(x|c_k)$ for both classes that obey the normal distribution, and all inputs are independent which is the case for a naïve Bayes classifier. The conditional probability density for each class is written using the chain rule as

$$p(x|c_k) = \prod_{i=1}^{D} \frac{1}{N_k} \sum_{j=1}^{N_k} \frac{1}{\sigma_{i,k}\sqrt{2\pi}} e^{-0.5\left(x_i - x_i^j\right)^2/\sigma_{i,k}^2} \tag{2}$$

where D is the dimension of the design space and x_i^j is the jth training point. $\sigma_{i,k}$ is a tunable parameter that shapes the normal distribution in the ith dimension of the design space for the class k. Using smaller $\sigma_{i,1}$ values means a more conservative design that avoids the misclassification type that classifies infeasible designs as feasible ones.

The classifier assigns the untested input x to the class that yields the maximum posterior probability according to Eq. (1), i.e., a design is feasible if $p(c_1|x) > p(c_2|x)$. However, when the number of data points belongs to one class is much more than the others,

the untested input x is assigned to the class that yields the maximum weighted posterior probability which is $w_k p(c_k|x)$. w_k is the loss factor and is introduced to reduce misclassification [11].

3.3 Gaussian Process Regression. GPR models are nonparametric kernel-based stochastic models that map the input x to its response y. The model is assumed to have multivariate Gaussian distributions for all its finite dimensions, which is mathematically described as

$$y \sim GP(\mu, \sigma^2), \quad \mu(x) = H(x)\beta, \quad \sigma^2 = \tau^2 r(x - x_i, \theta) \tag{3}$$

where $\mu(.)$ is the mean function, $\sigma(.)$ is the covariance function, $H(.)$ is the trend function that consists of a set of basis function of inputs x, $r(.,.)$ is the spatial correlation function and depends on the spatial distance between two inputs $x - x_i$, β, θ, and τ are the hyperparameters to be estimated in the training process of model. The prior of β is considered as Gaussian, $\beta \sim GP\ (b, B)$.

Based on the Bayes' theorem, the unobserved response y^* for a given input x^* can be predicted using the observed data pairs (y, x) as

$$E(y^*) = H_{y^*}^T \beta + \psi_{y,y^*}{}^* \psi_{y,y^*}^{-1} \left(Y - H_y^T \beta \right) \tag{4}$$

where ψ_{y,y^*} is a row vector that has its ith element as $\sigma^2(x–x^*)$ and $\psi_y = \sigma^2(x_i–x_j)$.

The prediction variance is

$$Var(y^*) = \psi_{y^*} - \psi_{y,y^*} \psi^{-1} \psi_{y,y^*}^T + R^T \left(B^{-1} + H_y K_y^{-1} H_y^T \right)^{-1} R \tag{5}$$

where $\beta = (B^{-1} + H_y K_y^{-1} H_y^T)^{-1} (H_y K_y^{-1} Y + B^{-1} b)$ and $R = H_y^* – H_y K_y^{-1} K_{y,y^*}$. The selection of spatial correlation function $r(.,.)$, also called the kernel function, has a significant influence on the accuracy of prediction. Common choices for the kernel function include the exponential kernel, Matern kernel, etc.

4 Data-Driven Design Space Exploration and Exploitation

In this section, a data-driven model-based design exploration and exploitation framework for DfAM is introduced. As shown in Fig. 3, BNC and GPR models are constructed to support the design space exploration and exploitation stages, respectively. These models are constructed based on one training dataset that is continuously refined through the design process. The initial dataset is created by high-fidelity computer simulations using a global sampling approach, and more high-fidelity data are added later using a local sampling approach that is based on a GPR model-assisted MCMC method.

4.1 Data-Driven Design Space Exploration. In design space exploration, the Bayesian network classifier is used as a tool to identify the solution set that satisfies the design target. The proposed workflow is summarized in Algorithm 1 and details about each step are described here.

First, DoE methods are used to generate a sampling plan S^1 ($S_i^1 \rightarrow \mathbb{R}^k$, $i = 1, \ldots, n$), which includes n design points for k-dimensional design space. Since the inclusion of more design variables results in an increase of computational cost, sensitivity analyses are used to determine these k design variables. As discussed, the Latin hypercube sampling method, a space-filling DoE, is selected to sample the design space. This sampling method maximizes the minimum distance among the samples S_i^1 in the design space.

Then, training data, including design points and their performance (S^1, Y^1), are obtained by conducting high-fidelity simulations at each design point S_i^1. By comparing its performance with the design target, each design point S_i^1 is labeled as either a feasible or an infeasible design, denoted as C_i^1. If the satisfactory performance region is changed, this labeling process is repeated, and the training data are updated. This ensures a rapid back-propagation from the performance space to the design space. Given a training dataset (S^1, C^1), a Bayesian Network Classifier is built to fit the data as closely as possible.

Next, a new sampling plan S^{full} is obtained by uniformly dividing the k-dimensional design space into N^k points which are equidistant in each dimension. The feasibility C^{full} of design points in S^{full} is obtained using the trained BNC. Instead of searching for a single optimal solution, this method searches and highlights all promising regions. The landscape of the design space can be visualized by multidimensional data visualization tools, e.g., the tile plot, nested plot, and city plot, or by dimensional reduction methods, e.g., t-SNE.

Algorithm 1 Data-driven design space exploration

1.	DoE $\rightarrow S^1$	% Sample the design space with a DoE method
2.	HF(S^1) $\rightarrow Y^1$	% Conduct high-fidelity simulations to evaluate performance
3.	Classify(Y^1) $\rightarrow C^1$	% Classify the performance into feasible and infeasible
4.	fit_bnc(S^1, C^1) $\rightarrow$ BNC	% Train a Bayesian network classifier
5.	DoE(N) $\rightarrow S^{\text{full}}$	% Divide the design space into equidistant points by BNC
6.	Prd (BNC, S^{full}) $\rightarrow C^{\text{full}}$	% Predict the feasibility of each design
7.	Visual (S^{full}, C^{full})	% Visualize the landscape of design space

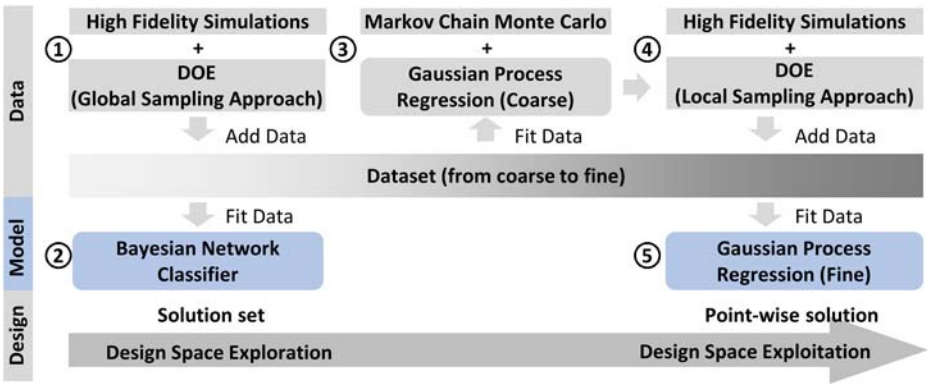

Fig. 3 The proposed data-driven framework for design exploration and exploitation. Design exploration (item 1–2) is discussed in Sec. 4.1 and design exploitation (item 3–5) is discussed in Sec. 4.2.

The use of BNC offers a rapid method to update feasible design regions for changes of ranged targets in the performance space. For example, in the wire arc additive manufacturing process, the bead height is controlled by two process parameters: the scan speed and wire feed rate. As shown in Fig. 4, the designer can first define an initial satisfactory region (e.g., range 1: 1.7–2.3 mm for the bead height) in early-stage design, and the corresponding feasible design region is determined with the BNC method. With more information given, the satisfactory region might narrow down from the indicated range 1 to range 2 and then to range 3. Using the BNC method, these changes can be reflected as narrowed feasible design regions.

Also, the BNC-based method can be used to explore the design space (also called the trade space) for multiobjective design problems. In addition to the bead height, the bead width is also set as an objective (4.3–4.9 mm) to the above-described design problem, as shown in Fig. 5. Feasible design regions for each design target are identified first. Then, feasible design regions that mutually satisfy two targets are obtained as the intersection between these two regions.

4.2 Data-Driven Design Space Exploitation. In the design space exploitation stage, optimization is used to search for a pointwise optimal design. Since intensive design evaluations are common in optimization, Gaussian process regression models are utilized as evaluation functions. However, the initial dataset that was created by a space-filling algorithm, a global sampling approach, in the design exploration stage needs to be refined at regions of interest to increase its local accuracy. A local sampling approach, the Markov Chain Monte Carlo-based resampling method, is introduced in Sec. 4.2.1. Based on the refined dataset, a GPR model-based design space exploitation method is presented in Sec. 4.2.2.

4.2.1 Markov Chain Monte Carlo Based Resampling. New design points are determined through a Bayesian inverse method: the Markov Chain Monte Carlo method. According to Eqs. (6) and (7), the Gaussian process regression models give us the statistical model in the form:

$$\gamma_i = f_i(\mathbf{x}) + \xi \tag{6}$$

where ξ is identical independent measurement noise with variance ν.

The training data S^1 constitutes our knowledge about the inputs prior to obtained observation Y^1 (prior uniform distributions). From the Bayesian perspective of input estimation, one can define the likelihood function as

$$L(x|S^1) = \frac{1}{(2\pi v^2)^{n/2}} e^{-SS/(2v^2)} \tag{7}$$

where

$$SS = \sum_{i=1}^{n} |\gamma_i - f_i(x)|^2 \tag{8}$$

is the sum of squared errors. The posterior density for the inputs given the observations is

$$p(x|S^1) \propto L(x|S^1) p_0(x) \tag{9}$$

where $p_0(x)$ is the initial distribution of inputs.

The posterior density in Eq. (9) is provided up to a normalization constant. Thus, a Markov chain, whose stationary distribution is the posterior, can be constructed to avoid computing. To construct such a Markov chain, one prominent approach is the delay rejection adaptive metropolis (DRAM) method [28]. DRAM generates a chain of design samples, which represents the distributions of inputs after observations. This chain also provides the marginal density function for each input. Sets of a one-dimensional orthogonal polynomial are constructed for the marginal density of each input. The roots of maximum order (e.g., 3-order) orthogonal polynomial are used as new sampling points for corresponding inputs [29]. The sparse grid or tensor grid constructed from inputs is used as the refined sampling plan S^2 to guarantee its filling property.

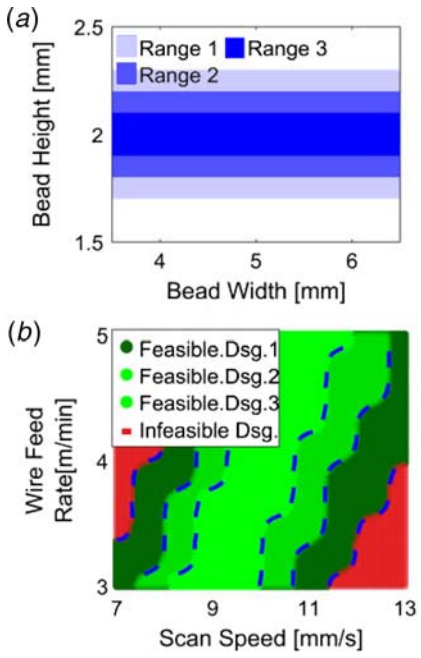

Fig. 4 An example of using BNC to examine the influence of changes in the satisfactory region on feasible design regions: (*a*) defined satisfactory regions for the bead height, range 1: 1.7–2.3 mm, range 2: 1.8–2.2 mm, range 3: 1.9–2.1 mm and (*b*) corresponding feasible design regions

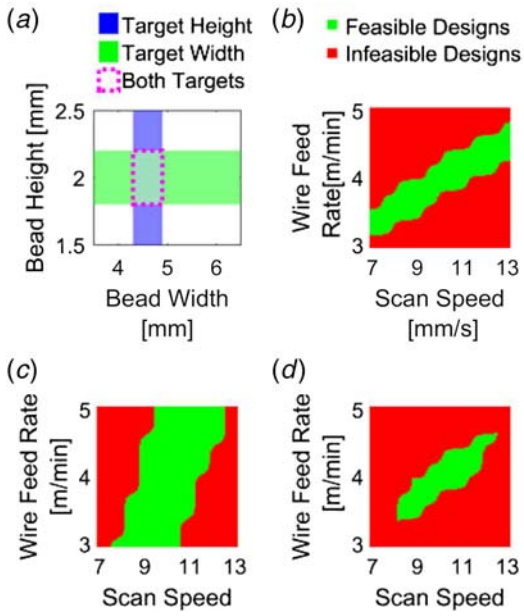

Fig. 5 An example of using BNC for design exploration for a multiobjective design problem: (*a*) design targets for bead heights and widths; (*b*) designs satisfy height targets; (*c*) designs satisfy width targets; and (*d*) designs satisfy both targets

It should be noted that the DRAM method updates the covariance matrix of the input for every k_0 time step which is different from the standard MCMC method with invariant covariant matrix V. Moreover, the proposal distribution is narrowed in the delayed rejection step which increases mixing of the chain. The use of Gaussian process regression model significantly reduces computational time because the chain generation from DRAM method requires extensive evaluations.

4.2.2 Gaussian Process Regression Model-Based Design Space Exploitation. The design space exploitation method based on the MCMC method and GPR models is summarized in Algorithm 2 and explained as follows:

Algorithm 2 Data-driven design space exploitation

1.	$S = S^1$, $Y = Y^1$	% Initialize dataset from design space exploration
2.	fit_gpr(S, Y) $\rightarrow$ GpMdl^1	% Train an initial Gaussian process regression model
3.	MCMC (Y^*,GpMdl^1) $\rightarrow$ dist(S)	% Identify distributions in the design space by the MCMC method
4.	Resamp (dist(S)) $\rightarrow S^2$	% Sample the promising distribution in the design space
5.	HF (S^2) $\rightarrow Y^2$	% Conduct high-fidelity simulations to evaluate responses
6.	$S^2 \cup S \rightarrow S$, $Y^2 \cup Y \rightarrow Y$	% Update dataset
7.	fit_gpr(S, Y) $\rightarrow$ GpMdl^2	% Train a refined Gaussian process regression model
8.	Opt(Y_i*, GpMdl^2) $\rightarrow S^*$	% Search for an optimized design using GPR model-based optimization

First, the training dataset created in the design space exploration (S^1, Y^1) is utilized as the initial dataset. Then, an initial Gaussian process regression model GpMdl1 is constructed to fit the coarse training data (S, Y). Next, the MCMC sampling method is used to sample regions that potentially include optimal designs. A new dataset (S^2, Y^2) is generated by evaluating new samples through high-fidelity simulations and adding them to the training dataset (S, Y). Next, a refined Gaussian process regression model GpMdl^2 is constructed to fit the refined training dataset (S, Y). To search for an optimal design, the GPR model is used as an evaluation function in general optimization routines which are widely used in engineering design [30]. Depending on the properties of given problems, different optimizers, e.g., gradient-based or gradient free algorithms, can be utilized. For AM-related designs that are often multimodal problems, global optimizers, e.g., genetic algorithms, that start from multiple locations from the design space often have better performance than gradient-based methods. For general design cases, designers should compare the performance of different optimizers and select the most effective one.

5 Case: Ankle Brace Design

In this section, the proposed design methods are applied to the design process of an additively manufactured ankle brace that has tailored stiffness requirements. This case exemplifies the utilization of structure-property relationships in embodiment design and detailed design. The ankle brace is to be manufactured with a stiff polymer material and using a material jetting process.

5.1 Design Problem Statement. Ankle braces are widely used orthoses in rehabilitation processes that immobilize the ankle joint while allowing it to heal from injuries such as acute sprains. According to studies [31], optimally designed ankle braces can adaptively adjust their allowable loading conditions and range of motions for joints along the course of recovery to ensure enough mechanical stimulations for tissue healing while avoiding extreme load conditions. Designs that fail to consider these factors can result in a chronic ankle joint instability. Two primary design factors of the ankle brace are the material selection and geometric structure design. In this study, we only consider the design of the geometric structure, as the AM process offers a cost-effective and rapid method to manufacture such tailored and complex geometry.

In this study, the ankle brace is designed as a two-dimensional (2D) structure, which does not need extra support structures in the additive manufacturing process and therefore reduces material wastes, compared with manufacturing the brace in its as-worn shape. As shown in Fig. 6, a CAD model of a human foot obtained by three-dimensional scanning is flattened as the design domain. The primary design target is to achieve the required motion range in all three directions by infilling the overall brace geometry with small scale geometric structures. One typical range of motions during the recovery process found from the literature [32,33] is listed in Table 4.

The domain is further divided into three regions according to their different contributions for limiting the range of motions in three directions. The ankle joint is considered as a ball joint that has its pivot point located at the origin of the defined coordinate, as depicted in Fig. 6(*a*). To specify design requirements for each region, the equilibrium of moments is constructed regarding the pivot point. To simplify the analysis, only axial deformations in two orthogonal directions are considered. More complicated deformations can be decomposed into these two directions. As shown in Fig. 6(*b*), the stiff and soft directions are denoted as directions 1 and 2, respectively. By solving the equilibrium of moments,

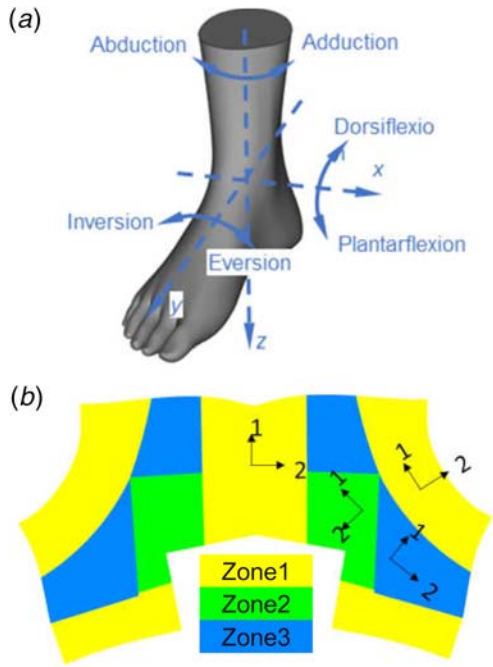

Fig. 6 (*a*) A scanned foot model and its coordinate system and (*b*) a 2D ankle brace that is flattened from the scanned foot model

Table 4 One set of range of motions and maximum torque for an ankle joint

	Range of motion	Maximum torque
X	± 20 deg	20 Nm
Y	± 5 deg	17.5 Nm
Z	± 5 deg	17.5 Nm

forces required for each region are obtained. Given the original geometry and allowable strain, the stress–strain requirements for each region are specified as listed in Table 5.

To tailor the stress–strain response of each zone, we select a type of flexible lattice structure, which we refer to as the horseshoe structure, as the basic design unit for populating the design domain. The horseshoe structure is highly stretchable [34] and has a nonlinear stress–strain response that is tunable by the design of its geometric structure. As shown in Fig. 7, the geometric structure is defined by five design variables: length L, radius R, width W, and angles α and β. The horseshoe structure is to be fabricated by the Stratasys® Polyjet J750 machine using a material jetting process due to its high resolution (27 μm). In addition, the Vero Cyan material, a stiff photopolymer (Young's modulus: ~1.7 GPa and Poisson's ratio: ~0.5) from Stratasys®, is to be used in this fabrication process.

The use of the horseshoe structure brings two advantages. First, its nonlinear J-shape stress–strain response, which is similar to the mechanical behavior of biological soft tissues, requires only small efforts to move the ankle until it reaches the maximum allowable motion range as shown in Fig. 7(*b*). Also, the anisotropic mechanical property allows different ranges of motions in two different directions. In Sec. 5.2, we determine the feasible range of these variables using the proposed design exploration algorithm. Then, one optimal design is found using the proposed design exploitation algorithm in Sec. 5.3.

5.2 Embodiment Design. Embodiment design utilizes the proposed design exploration algorithm to identify feasible designs. In this section, we only demonstrate the design exploration process for zone 1, and this approach can be followed in the design of rest zones.

First, the Latin hypercube sampling method is utilized to generate the sampling plan S^1 that consists of 200 design points distributed in a five-dimensional design space, which is defined in Table 6. To characterize their stress–strain responses, all designs are evaluated through FE analyses using ABAQUS/STANDARD (Dassault Systèmes®, 2017). This study considers the in-plane deformation only, and the structure is therefore modeled as 2D beams using B32H elements. To avoid edge effects, a square matrix with a sufficiently large number of horseshoe unit cells (5 × 5) is used in the simulation. Nodes on the bottom edge of the horseshoe matrix are fixed with an encastre boundary condition; meanwhile, a tensile load is applied through a displacement control of nodes on the top edge of the horseshoe matrix. Stress–strain responses Y^1 are obtained for the horseshoe structure in two directions. The prescribed workflow that includes DoE, FE analysis, and post-processing has been fully automated with an in-house developed toolkit in MATLAB (The MathWorks®, Inc., 2012).

The design tolerance range, which is the maximum deviation from the target defined in Table 5 that an acceptable design can have, is set to ± 0.05 MPa. All evaluated designs are labeled according to this criterion. Training datasets (S^1, C^1) are collected based on their performance in two directions. Next, two Bayesian network classifiers, BNC1 and BNC2, are trained to fit the training datasets for directions 1 and 2, respectively. To examine the landscape of the entire design space, an 8^5 grid is generated, and the feasibility of all design points C^{full} is predicted through the two classifiers. Designs that satisfy targets in each direction are identified first. To visualize the high-dimensional design space, feasible designs are shown with parallel coordinate plots in Fig. 8. As discussed, by intersecting feasible design regions for targets in each direction, designs that mutually satisfy targets in both directions are identified. To test and validate the proposed method, high-fidelity FE simulations are utilized to evaluate all 19 design points in the identified feasible regions, among which 3 design points are infeasible designs according to their performance from simulations. The misclassification rate is computed as 15.79% and can be further improved with a larger training dataset if extra computational budgets are allowed.

5.3 Detailed Design. In detailed design, the optimal design needs to be identified to meet a specific target rather than a range in the performance space. The proposed design exploitation algorithm is followed in detailed design. Training data (S^1, Y^1) from embodiment design are used as the initial dataset (S, Y), and the GPR model (denoted as the initial GPR model) GprMdl[1] is built based on this dataset. With the use of the MCMC resampling method, three distinct values are selected in each dimension, and a sampling plan with 35 design points is generated. The new dataset (S^2, Y^2) is added to the initial dataset (S, Y) to improve the confidence level of the GPR model around promising regions. Next, the GPR model (denoted as the refined GPR model) GprMdl[2] is retrained to fit the refined dataset and used in the

Table 5 Stress–strain requirements for each region

Zone #	Direction	Stress (MPa)	Strain (–)
Zone 1	1	0.47	30%
	2	0.24	10%
Zone 2	1	0.28	10%
	2	0.28	10%
Zone 3	1	0.43	10%
	2	0.49	10%

Table 6 Ranges for design variables of a horseshoe unit cell

Design variable	Width, W	Length, L	Radius, R	Angle, α	Angle, β
Design range	0.1–0.4 mm	0.1–0.2 mm	0.8–1.8 mm	0.1–1 rad	0.1–0.5 rad

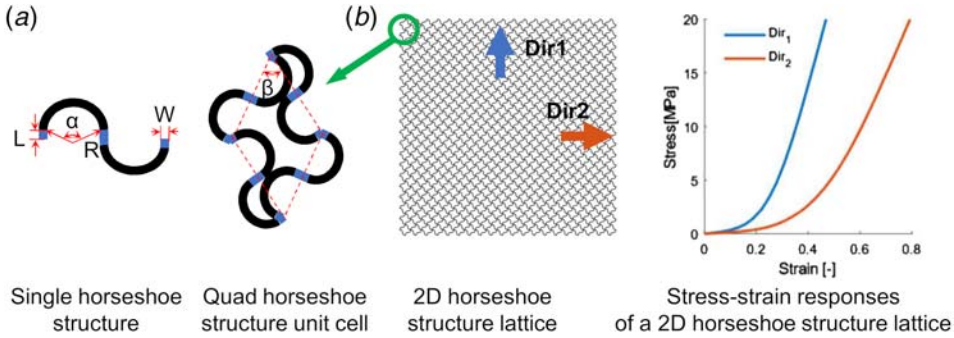

Fig. 7 (*a*) A quad horseshoe structure unit cell and its five design variables and (*b*) stress–strain responses of a quad horse shoe structure assembly in two directions

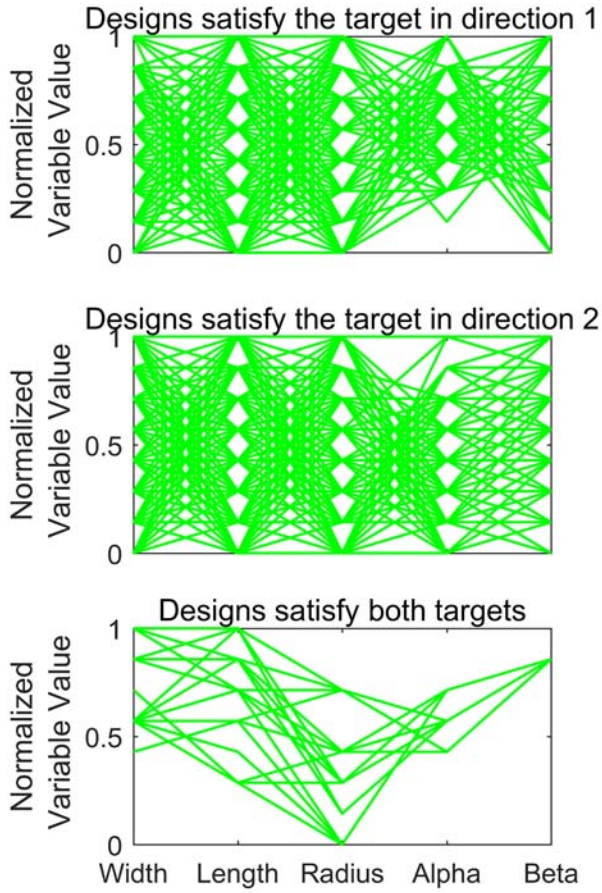

Fig. 8 Parallel coordinates plots for identified design regions that satisfy design targets of zone 1

optimization process as the evaluation function. The simplex method, one type of direct search optimizers, is used in the optimization routine. Optimal designs obtained using the refined GPR model-based optimization are listed in Table 7.

To validate the proposed method, optimal designs are also searched using initial GPR model-based optimization without resampling. Following the same exploitation method, optimal designs are also identified for zone 2 and zone 3, which have different design targets. High-fidelity FE simulations are used to assess the performance of designs obtained from two model types (initial and refined GPR). Their performance is measured with the root-mean-square error (RMSE), which is defined as $\text{RMSE} = \sqrt{\sum_{i=1}^{m} (y_i - \hat{y}_i)/m}$. m is the number of target stress–strain points. $\hat{y}_i$ and y_i are stress responses at a specific strain for the obtained design and target design, respectively. Their performance in terms of RMSE is compared in Table 7, and their stress–strain responses are shown in Fig. 9. In the design of all three zones, designs obtained from refined GPR model-based optimization show significantly lower RMSE values than designs obtained from initial GPR model-based optimization. As expected, the use of a refined sampling strategy for the dataset in design exploitation improves the performance of optimal designs found from optimization. It is also encouraging to see that the design exploration stage appears to have identified good design regions since design that met stress targets were found in design exploitation.

In addition, optimal designs for different targets of all three zones are found in design exploitation using the same initial dataset that was generated from design exploration. The example suggests that problems with more design targets, which is often the case in mass customization for additive manufacturing, can also be solved using the proposed approach since the local MCMC resampling method is employed to reuse global design information from design exploration for achieving different targets in the design exploration stage. Meanwhile, parallel computing methods can be used together with this design exploitation method to further reduce the product design time.

Table 7 Performance of designs identified by optimizations using initial and refined GPR models

		W (mm)	L (mm)	R (mm)	A (rad)	β (rad)	RMSE Dir.1 (MPa)	RMSE Dir.2 (MPa)
Zone 1	Initial GPR	0.272	0.135	1.144	0.577	0.442	96.5e − 4	15.1e − 3
	Refined GPR	0.274	0.131	1.007	0.637	0.437	2.77e − 4	3.03e − 3
Zone 2	Initial GPR	0.404	0.115	0.915	0.877	0.474	35.5e − 3	118e − 4
	Refined GPR	0.375	0.089	1.301	0.611	0.499	1.91e − 3	1.96e − 4
Zone 3	Initial GPR	0.166	0.179	0.695	0.352	0.478	2.00e − 2	69.6e − 3
	Refined GPR	0.210	0.148	0.760	0.427	0.493	1.21e − 2	4.66e − 3

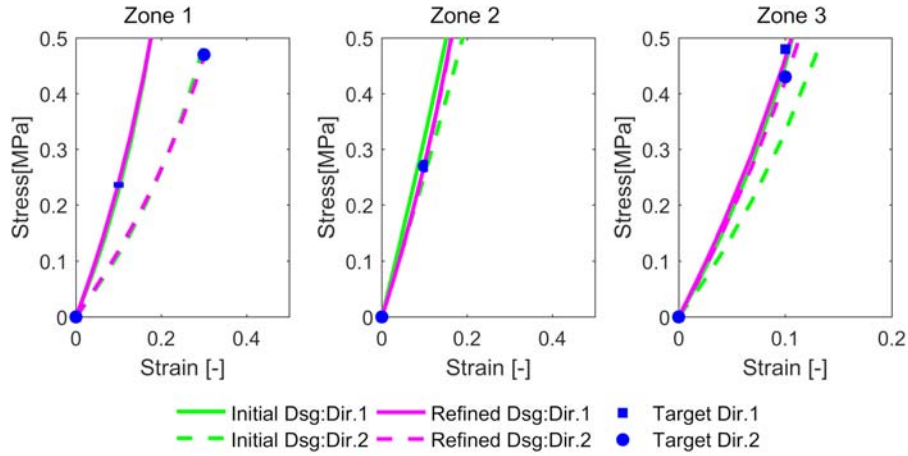

Fig. 9 FE analysis simulated stress–strain responses of identified optimal designs using initial GPR models and refined GPR models

Fig. 10 Fabricated ankle brace with optimized geometric structures

Once optimal designs are found, all zones in the 2D structure are populated and filled with these horseshoe designs. In the adjacent areas, boundaries of different designs are connected by joining open-ended struts to their nearest neighbors. The design is stored in STL files and fabricated using a material jetting process. As shown in Fig. 10, the fabricated part is folded to conform to the surface of the ankle.

6 Conclusions

In the context of design for additive manufacturing, a data-driven method has been presented for design search and optimization tasks in the design process. The characteristics of the design space for additively manufactured products were identified, and their requirements for design methods were summarized. These unique requirements necessitate a design method that is both rapid and tailored to different stages of design. Accordingly, data-driven models, instead of complex, physical-based high-fidelity models, were utilized as cost-effective tools to map design and performance spaces. In embodiment design, Bayesian network classifiers were used as the reasoning tool to identify feasible design regions and to explore the design space. Moreover, Gaussian process regression models were used in detailed design to search for a point-wise optimal design and to exploit the design space. Both models were constructed on one dataset that was initially created based on the Latin hypercube sampling method and then refined with more data that sampled with the MCMC sampling method. The method was demonstrated in the design case of an ankle brace that includes tailored horseshoe structures in different regions to achieve stiffness requirements in the rehabilitation process. The optimal designs found through the proposed two-step approach were evaluated through high-fidelity FEA simulations and demonstrated better performance than the design identified from the standalone exploitation approach.

The proposed design method utilizes a two-step data-driven approach to tackle the lack of integrated methods in the design process to link design exploration and exploitation, which is a research gap observed in many engineering design problems. The proposed method is therefore generally applicable to other applications and not limited in scope to DfAM.

One should note that the validation example with the ankle brace design problem includes most identified design scenarios required for the design tool, i.e., supporting a high-dimensional design space, supporting mass customization, and supporting the multiobjective optimization, except for the multidisciplinary design case. However, due to its effectiveness, this data-driven method is also a promising solution to design simultaneously the products, its materials, and their manufacturing processes using multidisciplinary optimization. In future work, the proposed design methods will be applied to navigate process-structure-property relationships at multiple scales as defined in the design problem formulation for DfAM [1].

Funding Data

- Digital Manufacturing and Design (DManD) Research Center at the Singapore University of Technology and Design (RGDM1710205) supported by the Singapore National Research Foundation.

Nomenclature

Abbreviations

2D = two-dimensional
AM = additive manufacturing
BNC = Bayesian network classifier
CAD = computer-aided design
DfAM = design for additive manufacturing
DfM = design for manufacturing
DoE = design of experiment
DRAM = delay rejection adaptive metropolis
FE = finite element
GPC = Gaussian process classifier
GPR = Gaussian process regression
MCMC = Markov chain Monte Carlo
PSP = process-structure-property
RMSE = root-mean-square error
RSM = response surface method
SLM = selective laser melting
STL = stereolithography

References

[1] Rosen, D. W., 2014, "Research Supporting Principles for Design for Additive Manufacturing," Virtual Phys. Prototyp., **9**(4), pp. 225–232.
[2] Rosen, D. W., 2007, "Computer-Aided Design for Additive Manufacturing of Cellular Structures," Comput. Aided. Des. Appl., **4**(5), pp. 585–594.
[3] Pahl, G., Beitz, W., Feldhusen, J., and Grote, K.-H., 2007, *Engineering Design: A Systematic Approach*, Springer-Verlag London, London.
[4] Rosen, D. W., 2015, "A Set-Based Design Method for Material-Geometry Structures by Design Space Mapping," ASME Design Automation Conference, Boston, MA, Aug. 2–5, ASME Paper No. DETC2015-46760.
[5] Tapia, G., Khairallah, S., Matthews, M., King, W. E., and Elwany, A., 2018, "Gaussian Process-Based Surrogate Modeling Framework for Process Planning in Laser Powder-Bed Fusion Additive Manufacturing of 316L Stainless Steel," Int. J. Adv. Manuf. Technol., **94**(9–12), pp. 3591–3603.
[6] Li, J., Jin, R., and Yu, H. Z., 2018, "Integration of Physically-Based and Data-Driven Approaches for Thermal Field Prediction in Additive Manufacturing," Mater. Des., **139**, pp. 473–485.
[7] Kamath, C., 2016, "Data Mining and Statistical Inference in Selective Laser Melting," Int. J. Adv. Manuf. Technol., **86**(5–8), pp. 1659–1677.
[8] Yan, W., Lin, S., Kafka, O. L., Lian, Y., Yu, C., Liu, Z., Yan, J., Wolff, S., Wu, H., Ndip-Agbor, E., Mozaffar, M., Ehmann, K., Cao, J., Wagner, G. J., and Liu, W. K., 2018, "Data-Driven Multi-Scale Multi-Physics Models to Derive Process–Structure–Property Relationships for Additive Manufacturing," Comput. Mech., **61**(5), pp. 521–541.
[9] Morris, C., Bekker, L., Haberman, M. R., and Seepersad, C. C., 2018, "Design Exploration of Reliably Manufacturable Materials and Structures With Applications to Negative Stiffness Metamaterials and Microstereolithography," ASME J. Mech. Des., **140**(11), p. 111415.
[10] Matthews, J., Klatt, T., Morris, C., Seepersad, C. C., Haberman, M., and Shahan, D., 2016, "Hierarchical Design of Negative Stiffness Metamaterials Using a Bayesian Network Classifier," ASME J. Mech. Des., **138**(4), p. 041404.
[11] Shahan, D. W., and Seepersad, C. C., 2012, "Bayesian Network Classifiers for Set-Based Collaborative Design," ASME J. Mech. Des., **134**(7), p. 071001.
[12] Malak, R. J., Aughenbaugh, J. M., and Paredis, C. J. J., 2009, "Multi-Attribute Utility Analysis in Set-Based Conceptual Design," Comput. Des., **41**(3), pp. 214–227.
[13] Weiss, L. E., Amon, C. H., Finger, S., Miller, E. D., Romero, D., Verdinelli, I., Walker, L. M., and Campbell, P. G., 2005, "Bayesian Computer-Aided Experimental Design of Heterogeneous Scaffolds for Tissue Engineering," Comput. Des., **37**(11), pp. 1127–1139.
[14] Pacheco, J. E., Amon, C. H., and Finger, S., 2003, "Bayesian Surrogates Applied to Conceptual Stages of the Engineering Design Process," ASME J. Mech. Des., **125**(4), pp. 664–672.

[15] Williams, C. B., Mistree, F., and Rosen, D. W., 2011, "A Functional Classification Framework for the Conceptual Design of Additive Manufacturing Technologies," ASME J. Mech. Des., **133**(12), p. 121002.
[16] Unal, M., Miller, S. W., Chhabra, J. P. S., Warn, G. P., Yukish, M. A., and Simpson, T. W., 2017, "A Sequential Decision Process for the System-Level Design of Structural Frames," Struct. Multidiscip. Optim., **56**(5), pp. 991–1011.
[17] Chen, W., Allen, J. K., and Mistree, F., 1997, "A Robust Concept Exploration Method for Enhancing Productivity in Concurrent Systems Design," Concurr. Eng., **5**(3), pp. 203–217.
[18] Choi, H., McDowell, D. L., Allen, J. K., Rosen, D., and Mistree, F., 2008, "An Inductive Design Exploration Method for Robust Multiscale Materials Design," ASME J. Mech. Des., **130**(3), p. 031402.
[19] Sharpe, C., Morris, C., Goldsberry, B., Seepersad, C. C., and Haberman, M. R., 2017, "Bayesian Network Structure Optimization for Improved Design Space Mapping for Design Exploration With Materials Design Applications," Design Automation Conference, Cleveland, OH, Aug. 6–9, ASME Paper No. DETC2017-67643.
[20] Gaier, A., Asteroth, A., and Mouret, J.-B., 2018, "Data-Efficient Design Exploration Through Surrogate-Assisted Illumination," Evol. Comput., **26**(3), pp. 381–410.
[21] Larson, B. J., and Mattson, C. A., 2012, "Design Space Exploration for Quantifying a System Model's Feasible Domain," ASME J. Mech. Des., **134**(4), p. 041010.
[22] Couckuyt, I., Declercq, F., Dhaene, T., Rogier, H., and Knockaert, L., 2010, "Surrogate-Based Infill Optimization Applied to Electromagnetic Problems," Int. J. RF Microw. Comput.-Aided Eng., **20**(5), pp. 492–501.
[23] Simpson, T. W., and Mistree, F., 2001, "Kriging Models for Global Approximation in Simulation-Based Multidisciplinary Design Optimization," AIAA J., **39**(12).
[24] Qian, Z., Seepersad, C. C., Joseph, V. R., Allen, J. K., and Wu, C. F. J., 2006, "Building Surrogate Models Based on Detailed and Approximate Simulations," ASME J. Mech. Des., **128**(4), pp. 668–677.
[25] Chen, W., and Fuge, M., 2017, "Beyond the Known: Detecting Novel Feasible Domains Over an Unbounded Design Space," ASME J. Mech. Des., **139**(11), p. 111405.
[26] Wang, G. G., and Shan, S., 2007, "Review of Metamodeling Techniques in Support of Engineering Design Optimization," ASME J. Mech. Des., **129**(4), pp. 370–380.
[27] Simpson, T. W., Poplinski, J. D., Koch, P. N., and Allen, J. K., 2001, "Metamodels for Computer-Based Engineering Design: Survey and Recommendations," Eng. Comput., **17**(2), pp. 129–150.
[28] Haario, H., Laine, M., Mira, A., and Saksman, E., 2006, "DRAM: Efficient Adaptive MCMC," Stat. Comput., **16**(4), pp. 339–354.
[29] Ahlfeld, R., Montomoli, F., Belouchi, B., Belkouchi, B., and Montomoli, F., 2016, "Sparse Approximation Moment-Based Arbitrary Polynomial Chaos," J. Comput. Phys., **320**, pp. 1–16.
[30] Belegundu, A. D., and Chandrupatla, T. R., 1999, *Optimization Concepts and Applications in Engineering*, Cambridge University Press, New York.
[31] Thiele, F., Schuhmacher, S., Schwaller, C., Plüss, S., Rhiner, J., List, R., and Lorenzetti, S., 2018, "Restrictions in the Ankle Sagittal- and Frontal-Plane Range of Movement During Simulated Walking With Different Types of Orthoses," J. Funct. Morphol. Kinesiol., **3**(2), p. 21.
[32] Chen, J., Siegler, S., and Schneck, C. D., 1988, "The Three-Dimensional Kinematics and Flexibility Characteristics of the Human Ankle and Subtalar Joint—Part II: Flexibility Characteristics," ASME J. Biomech. Eng., **110**(4), pp. 374–385.
[33] Siegler, S., Chen, J., and Schneck, C. D., 1988, "The Three-Dimensional Kinematics and Flexibility Characteristics of the Human Ankle and Subtalar Joints—Part I: Kinematics," ASME J. Biomech. Eng., **110**(4), pp. 364–373.
[34] Jang, K. I., Chung, H. U., Xu, S., Lee, C. H., Luan, H., Jeong, J., Cheng, H., Kim, G. T., Han, S. Y., Lee, J. W., Kim, J., Cho, M., Miao, F., Yang, Y., Jung, H. N., Flavin, M., Liu, H., Kong, G. W., Yu, K. J., Rhee, S. I., Chung, J., Kim, B., Kwak, J. W., Yun, M. H., Kim, J. Y., Song, Y. M., Paik, U., Zhang, Y., Huang, Y., and Rogers, J. A., 2015, "Soft Network Composite Materials with Deterministic and Bio-Inspired Designs," Nat. Commun., **6**(1), pp. 1–11.